Supporting Information

Effect of ceramic-target crystallinity on metal-to-insulator transition of epitaxial rare-earth nickelate films grown by pulsed laser deposition

Jin San Choi[†,‡], Muhammad Sheeraz[†,‡], Jong-Seong Bae[§], Jun Han Lee[※], Joonhyuk Lee[₸], Jongmin Lee[‖], Sanghan Lee[‖], Hyoungjeen Jeen[₸], Yoon Seok Oh[※], Chang Won Ahn[†], and Tae Heon Kim[†,*]

†Department of Physics and Energy Harvest Storage Research Center (EHSRC), University of Ulsan, Ulsan 44610, Republic of Korea

§Busan Center, Korea Basic Science Institute, Busan 46742, Republic of Korea

※Department of Physics, Ulsan National Institute of Science and Technology (UNIST), Ulsan 44919, Republic of Korea

₸Department of Physics, Pusan National University, Busan 46241, Republic of Korea

‖School of Materials Science and Engineering, Gwangju Institute of Science and Technology, Gwangju 61005, Republic of Korea

*Correspondence to thkim79@ulsan.ac.kr

Hypothesis of our study

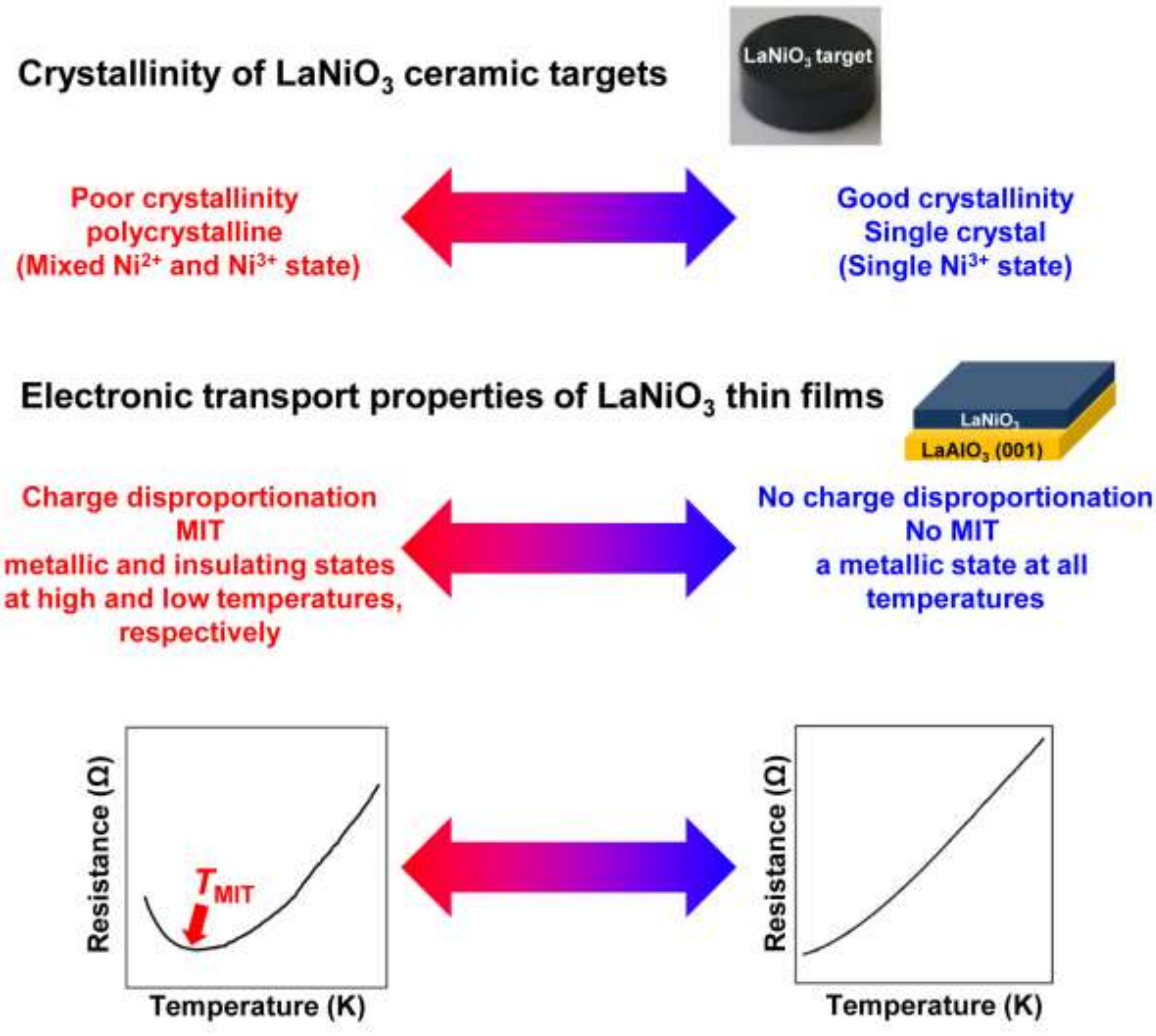

Supplementary Fig. S1. A schematic diagram of tuning of the metal-to-insulator phase transitions in $LaNiO_3$ thin films via the controlled crystallinity of ceramic targets in pulsed laser deposition (PLD).

Schematic illustrations of ceramic-target synthesis and thin-film growth in $LaNiO_3$

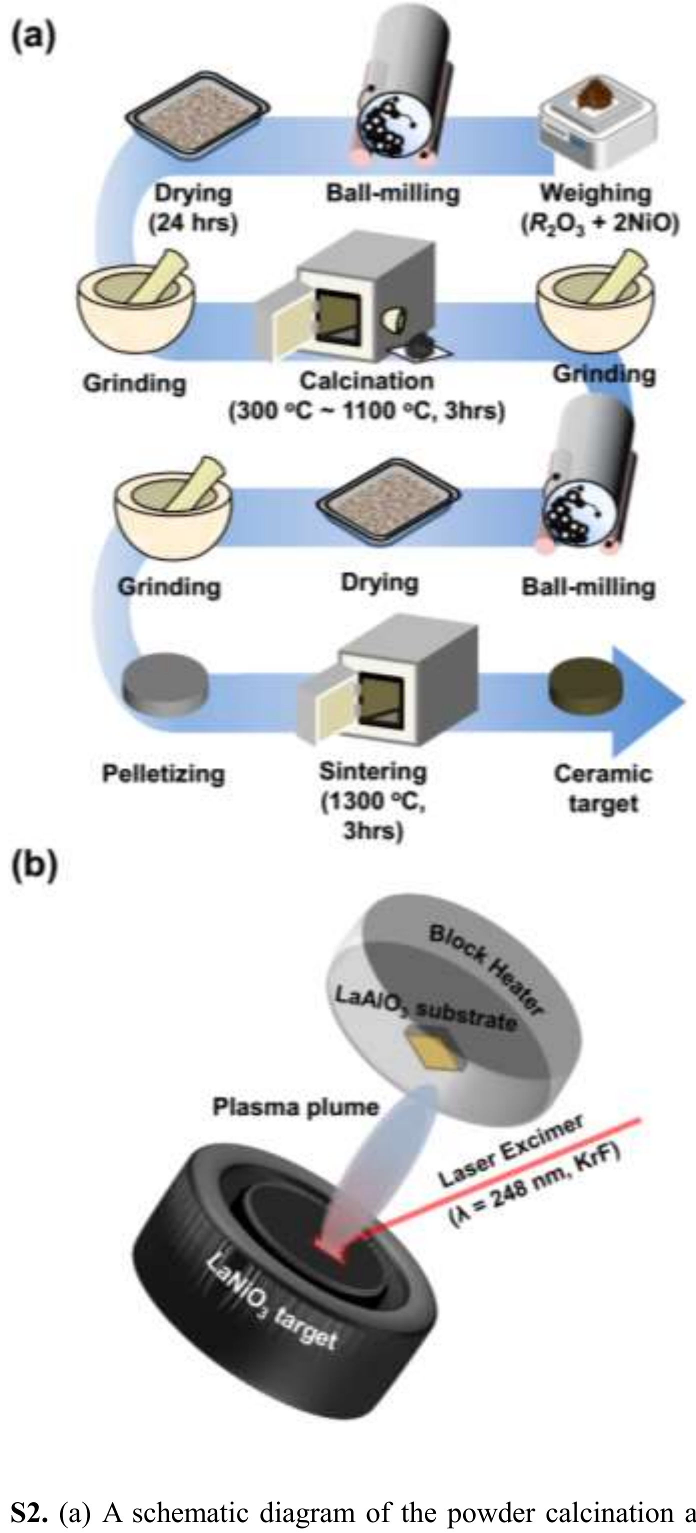

Supplementary Fig. S2. (a) A schematic diagram of the powder calcination and the ceramic-target synthesis in the solid-state-reaction process. (b) A schematic illustration of the pulsed laser deposition (PLD) growth of epitaxial $LaNiO_3$ (001) films.

Local elemental analyses of the as-sintered $LaNiO_3$ ceramic target using energy dispersive spectroscopy (EDS)

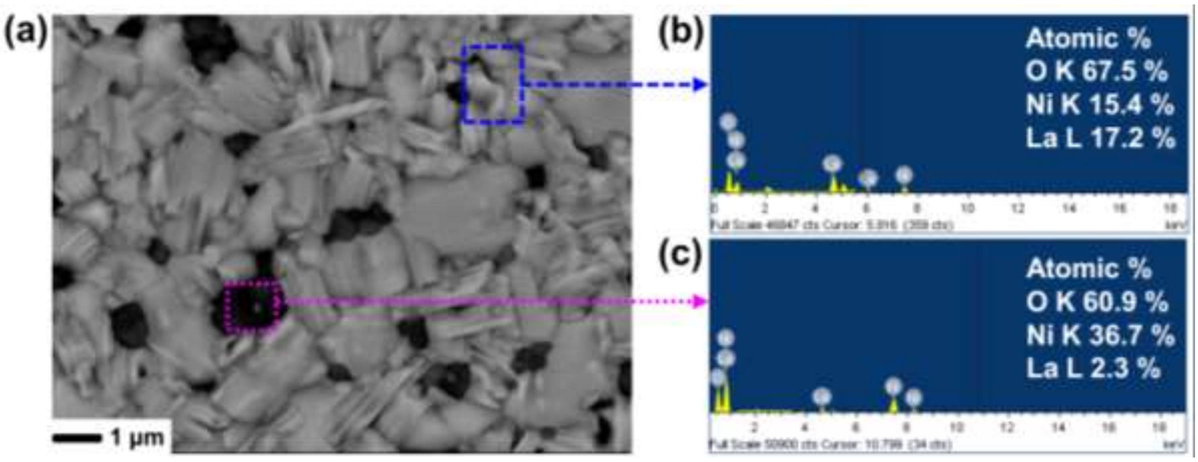

Supplementary Fig. S3. (a) The back-scattered surface image of a $LaNiO_3$ ceramic target measured by field emission-scanning electron microscope (FE-SEM). The local energy dispersive spectroscopy (EDS) of (b) the gray region [marked by the blue dashed rectangle], and (c) the black region [marked by the pink dotted square] in the back-scattered SEM image of (a). In the black region, the Ni content is exceedingly excessive, whereas the La content is very deficient.

The overall stoichiometry analyses on $LaNiO_3$ target surfaces (sintered after the calcination at 300 and 1000 °C)

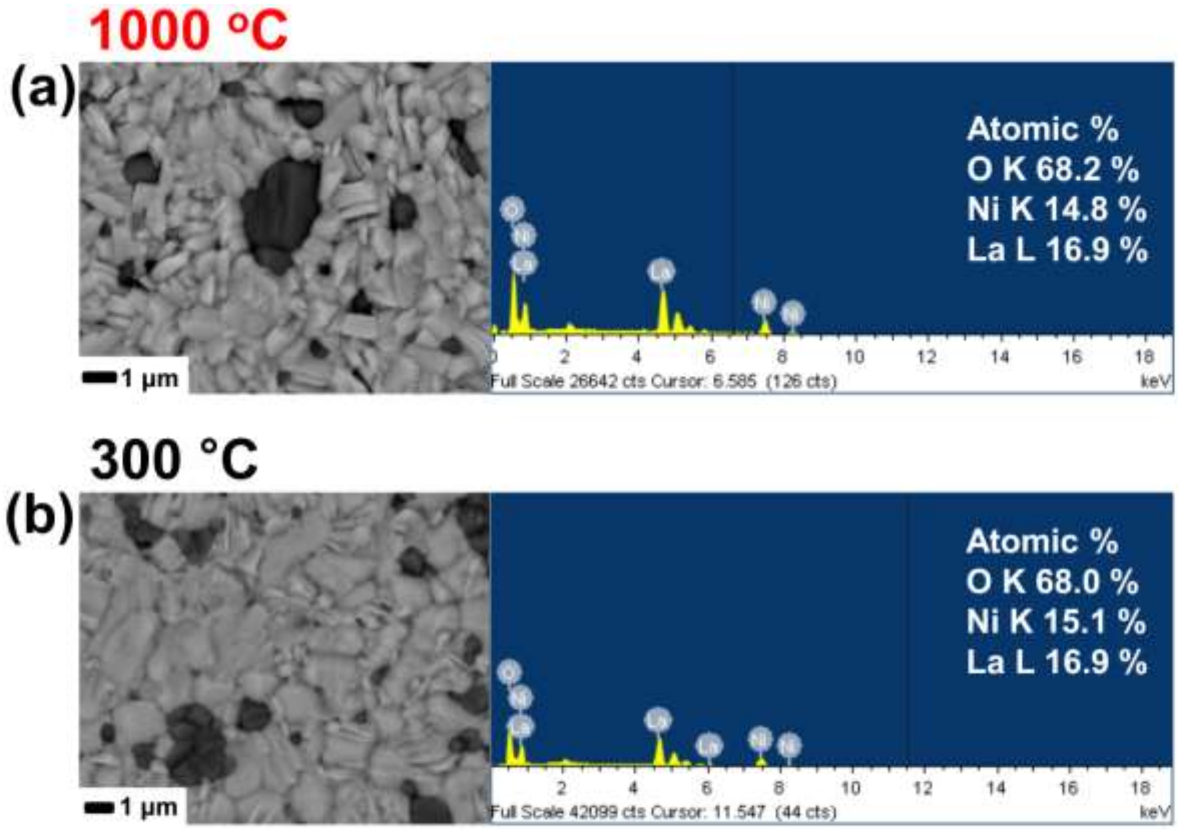

Supplementary Fig. S4. The back-scattered FE-SEM images and the corresponding EDS spectra of the as-sintered $LaNiO_3$ target surfaces after the high-temperature and low-temperature calcination at (a) 1000 and (b) 300 °C, respectively. The overall La and Ni contents between these two $LaNiO_3$ targets (calcined at 300 and 1000 °C) are identical within the measurement error.

Thickness estimation of epitaxial $LaNiO_3$ (001) films

We estimated the film thickness of epitaxial $LaNiO_3$ (001) films by simulating thickness fringes around the (001) Bragg peak in their X-ray diffraction (XRD) θ-2θ spectra, as shown in the Supplementary Figure S5. For the simulation of the measured XRD intensity (I) in the thickness fringes, we used the following formulas:

$$I(q_z) \propto \frac{\sin^2(q_z\ Nd/2)}{\sin^2(q_z\ d/2)} \tag{1}$$

$$q_z = L - Q_z \tag{2}$$

$$Q_z = \frac{4\pi}{\lambda} \sin\theta \tag{3}$$

where N represents the film thickness (the number of unit cells), d is the lattice d-spacing in the normal direction to the diffraction plane, λ is the X-ray wavelength (Cu Kα_1 = 1.5406 Å), and $L = \frac{4\pi}{\lambda}\sin\theta_B$ (Here, θ_B is the diffraction angle at the Bragg's condition). By comparing the experimental XRD data (the black solid curve) with the simulated thickness fringe (the blue dashed curve), we determined that the estimated thickness of an ultrathin $LaNiO_3$ (001) film is 10 unit cells, that is, ~3.84 nm.

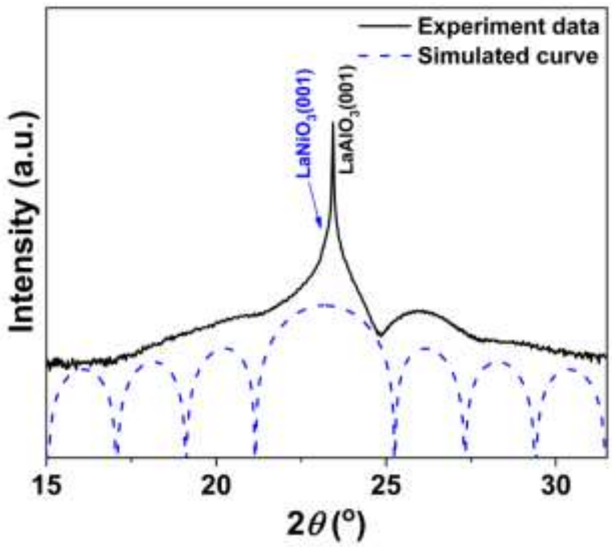

Supplementary Fig. S5. Estimating the film thickness in an ultrathin $LaNiO_3$ (001) film. The measured XRD intensity (the black solid curve) around the (001) Bragg peak is compared with the simulated intensity (the blue dashed curve) of the oscillating thickness fringes.

High-resolution reciprocal space mappings (RSMs) of the $LaNiO_3$ thin films

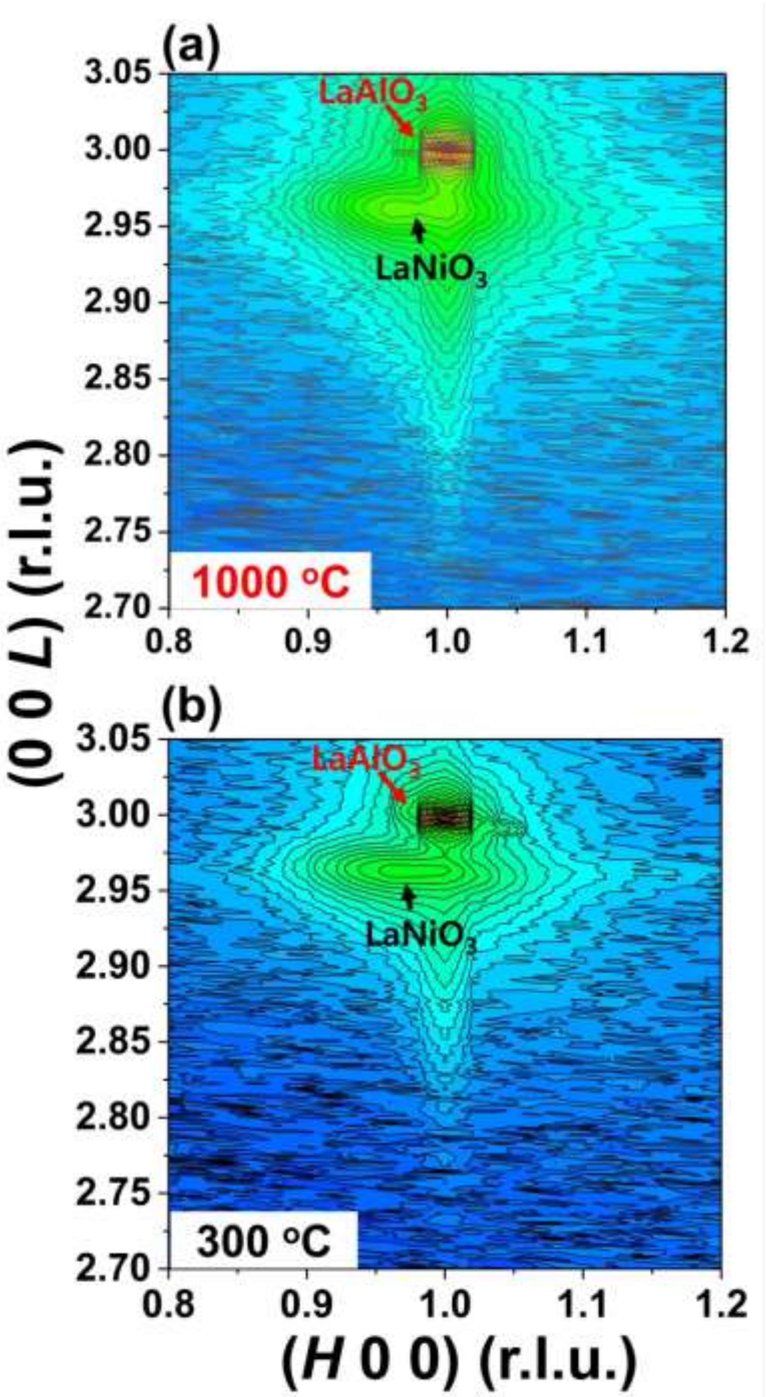

Supplementary Fig. S6. The RSMs of two epitaxial $LaNiO_3$ (001) films, synthesized from as-sintered $LaNiO_3$ ceramic targets after (a) high-temperature (1000 ˚C) and (b) low-temperature (300 ˚C) calcination, around the (103) Bragg peaks of the underlying $LaAlO_3$ substrates in pseudocubic notation. In (a) [(b)], the measured out-of-plane and in-plane lattice constants are about 3.834 (3.834) and 3.789 (3.789) Å, respectively.

The surface stoichiometry analyses of the as-grown $LaNiO_3$ thin films fabricated from different $LaNiO_3$ ceramic targets sintered after high-temperature (1000 °C) and low-temperature (300 °C) calcination

To examine the chemical stoichiometry of the as-grown $LaNiO_3$ thin films using EDS, we epitaxially grew two $LaNiO_3$ films on $SrTiO_3$ (001) substrates with two different $LaNiO_3$ ceramic targets. In $LaNiO_3$ films grown on $LaAlO_3$ (001) substrates, it is very difficult for us to estimate the accurate La content inside the $LaNiO_3$ film layer, because the incorporated La atoms in the $LaAlO_3$ substrates generate strong background signals in the raw EDS spectra. To avoid the strong background signals arising from the underlying substrate, we fabricated $LaNiO_3$ films on $SrTiO_3$ substrates composed of different cations (i.e., Sr and Ti elements).

The supplementary figure S7 shows the measured EDS spectra of epitaxial $LaNiO_3$ films grown on $SrTiO_3$ (001) substrates. Here, two $LaNiO_3/SrTiO_3$ (001) films were fabricated from two $LaNiO_3$ ceramic targets sintered after the high-temperature (1000 °C) and low-temperature (300 °C) calcination. However, the measured EDS intensity of the La and Ni atoms was very weak due to the dominant signals of the Sr and Ti atoms inside the $SrTiO_3$ substrate. Nevertheless, it is worthy of note that the atomic percentages of the La and Ni elements are nearly identical to 1.25 (2.19) and 1.24 (1.92) % in the $LaNiO_3/SrTiO_3$ (001) film deposited with the $LaNiO_3$ target after the high-temperature (low-temperature) calcination. This indicates that the La and Ni contents in the as-grown $LaNiO_3$ films are stoichiometric with no La or Ni vacancies.

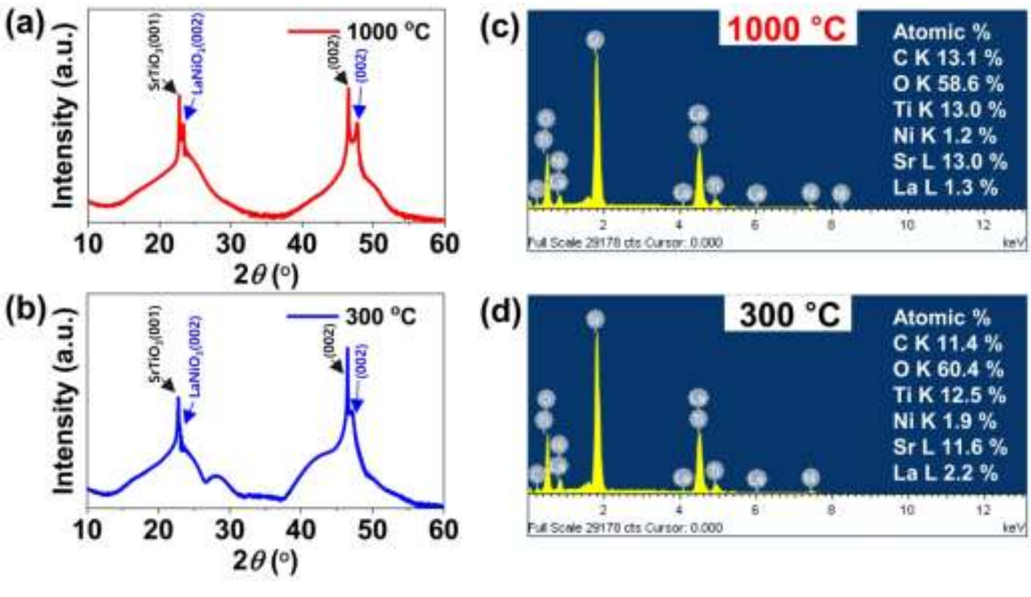

Supplementary Fig. S7. XRD θ-2θ scans of the as-grown $LaNiO_3/SrTiO_3$ (001) films fabricated from two $LaNiO_3$ ceramic targets sintered after the (a) high-temperature (1000 °C) and (b) low-temperature (300 °C) calcination. (c,d) The corresponding EDS spectra of the as-deposited $LaNiO_3/SrTiO_3$ (001) film surfaces in (a) and (b), respectively.

The surface morphology of the $LaNiO_3$ (001) thin film

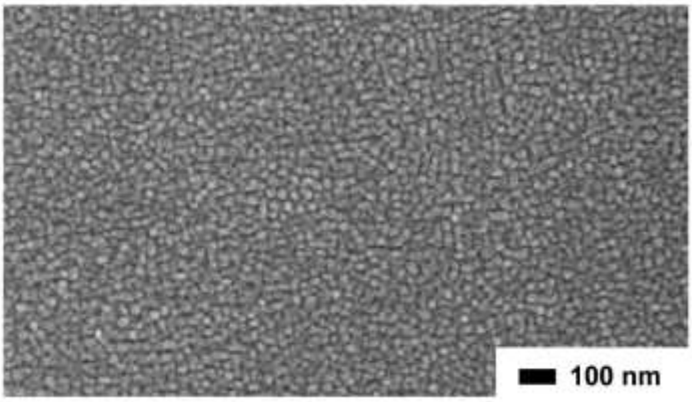

Supplementary Fig. S8. The FE-SEM image of the surface topography of the as-grown $LaNiO_3$ (001) thin film.

The electrical transport measurements of $LaNiO_3$ (001) thin films

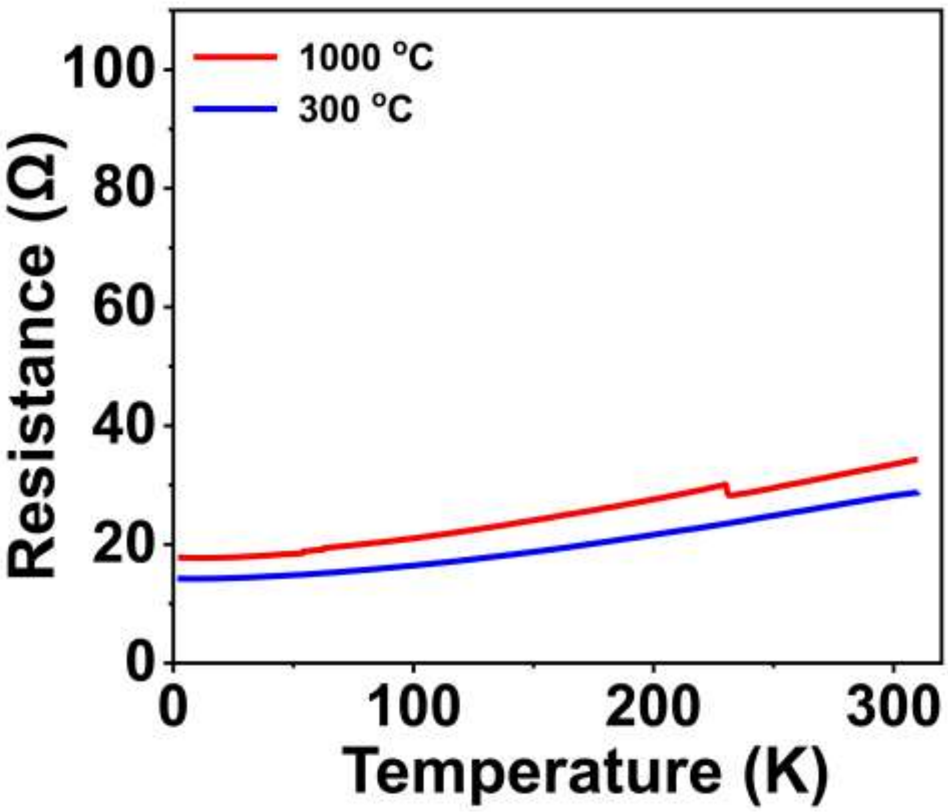

Supplementary Fig. S9. The temperature-dependent resistance of two $LaNiO_3$ (~10 unit cells) (001) films which are twice thicker than $LaNiO_3$ (~5 unit cells) (001) films used in Fig. 4(d).

Thickness-dependent transport behaviors of $LaNiO_3$ (001) thin films

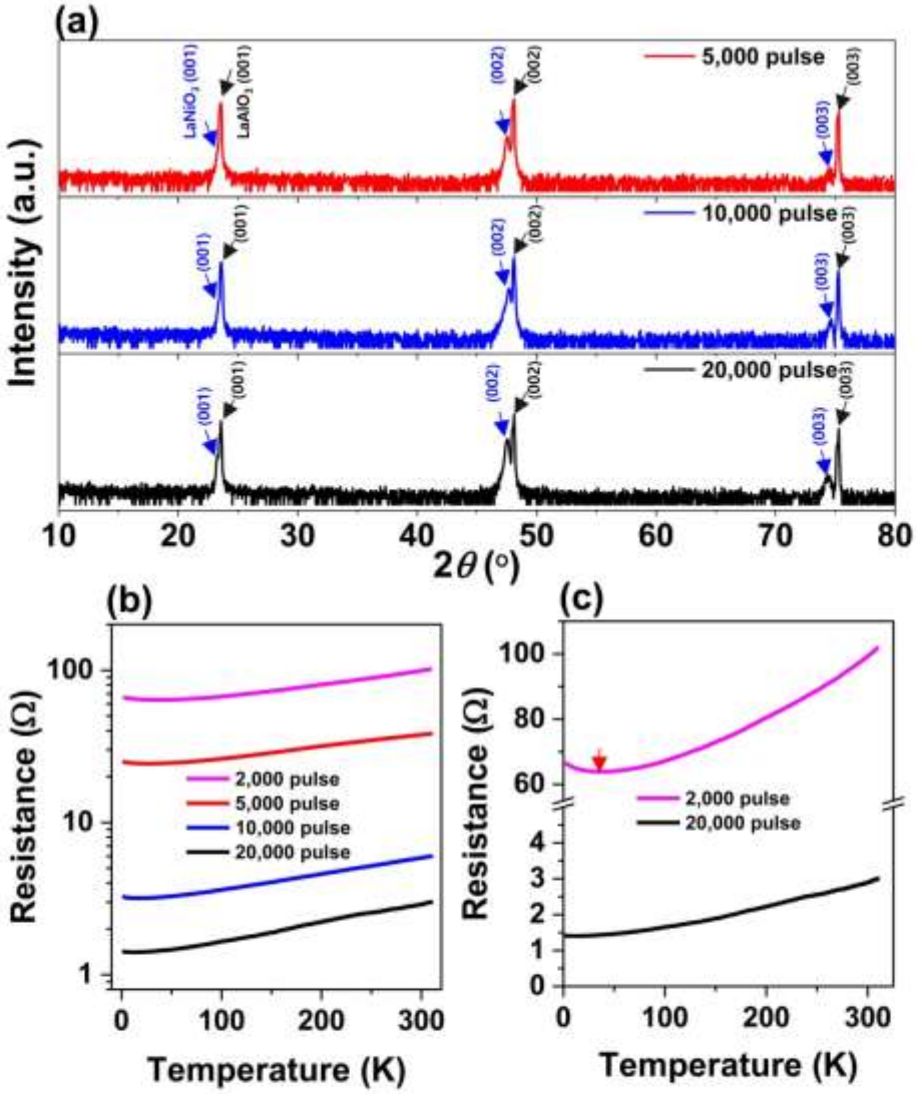

Supplementary Fig. S10. (a) XRD θ-2θ scans of epitaxial $LaNiO_3/LaAlO_3$ (001) films with different thickness. Here, the film thickness is manipulated by the number (N_{pulse}) of the applied laser pulses. (b) The thickness dependence of electrical transport properties of the as-grown $LaNiO_3/LaAlO_3$ (001) films. (c) A comparison of the transport properties between two $LaNiO_3$ films with different thickness. The thinner $LaNiO_3$ film (N_{pulse} = 2000 pulses) exhibits a metal-to-insulator transition (a red arrow), while the thicker $LaNiO_3$ film (N_{pulse} = 20000 pulses) is metallic at all temperatures.

The x-ray photoelectron spectroscopy (XPS) analysis of $LaNiO_3$ (001) thin films

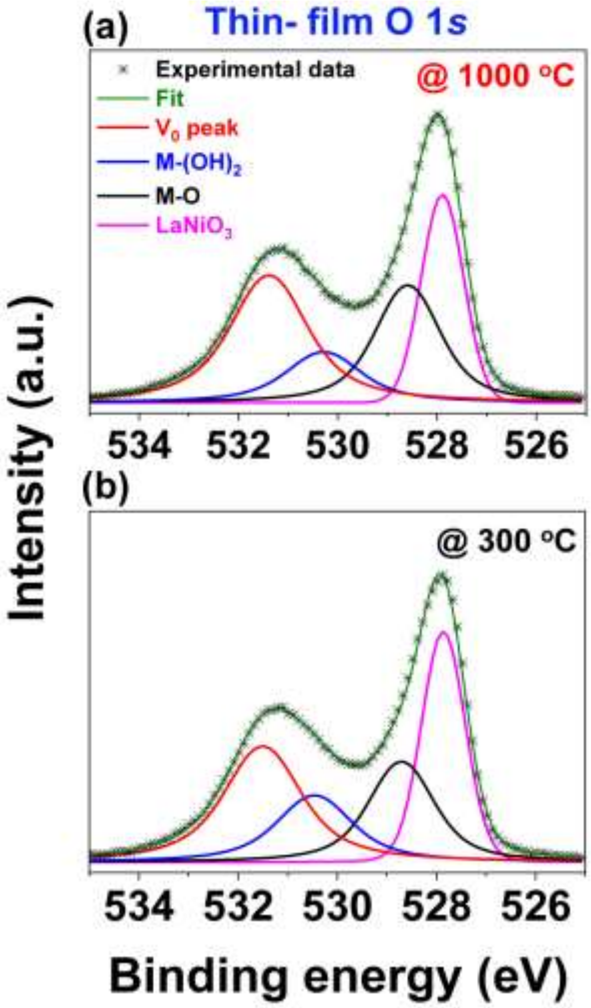

Supplementary Fig. S11. XPS spectra at the O 1s edge of two as-grown $LaNiO_3$ (001) films [the same samples used in Figs. 5(a) and 5(b)] fabricated from two different $LaNiO_3$ ceramic targets sintered after (a) high-temperature (1000 ˚C) and (b) low-temperature (300 ˚C) calcination. The red, blue, black, and magenta solid lines represent the fitted curves of the oxygen vacancy (V_O) peak, the metal hydrate (M-(OH)$_2$) peak, the metal oxide (M-O) peak, and the lattice oxygen peak in $LaNiO_3$, respectively.